

# Regular and Chaotic Dynamics in the Mean-Motion Resonances: Implications for the Structure and Evolution of the Asteroid Belt

**D. Nesvorný**

*Southwest Research Institute*

**S. Ferraz-Mello**

*Universidade de São Paulo*

**M. Holman**

*Harvard-Smithsonian Center for Astrophysics*

**A. Morbidelli**

*Observatoire de la Côte d'Azur*

---

This chapter summarizes the achievements over the last decade in understanding the effect of mean-motion resonances on asteroid orbits. The developments from the beginning of the 1990s are many. They range from a complete theoretical description of the secular dynamics in the mean-motion resonances associated with the Kirkwood gaps to the discovery of the three-body resonances and slow chaotic phenomena acting throughout the asteroid belt. Consequences arising from these results have required remodeling the process of asteroid delivery to the Earth-crossing orbits.

## 1. INTRODUCTION

It is evident from the plethora of studies of mean-motion resonances (MMRs) in the last decade that major advances have been made in this area, and these advances have broad consequences for our understanding of asteroids. An attentive observer of this branch of dynamical astronomy would have noted the following progress.

It was shown that bodies in the main MMRs with Jupiter (3:1, 4:1, 5:2) can reach very high orbital eccentricities (Ferraz-Mello and Klafke, 1991; Klafke et al., 1992; Saha, 1992). This result suggested that resonant bodies can be transported to Mars-, Earth-, and Venus-crossing orbits and then be efficiently extracted from the resonances due to the larger mass of the two latter planets. The cited works confirmed the pioneering findings of Wisdom (1982, 1983, 1985) on the Kirkwood gap at the 3:1 MMR with Jupiter and showed that very high eccentricities are frequent outcomes of the dynamics in MMRs on million-year timescales.

The progress in numerical modeling revealed another surprising alternative: Resonant asteroids can fall into the Sun (Farinella et al., 1993, 1994), as a consequence of their eccentricity approaching unity. The current state of our understanding of the removal of resonant bodies from the 3:1 MMR is that 65–70% are extracted by Earth and Venus, and 25–30% go directly into the Sun (Gladman et al., 1997).

The innovative seminumerical treatment of classical perturbation methods introduced by Henrard (1990) later allowed a global and realistic description of the secular dy-

namics in the main MMRs with Jupiter, taking into account the precession of Jupiter's orbit (Moons and Morbidelli, 1995). This supplied convincing evidence that the orbital evolution of simulated bodies toward the planet-crossing orbits is driven by chaotic secular resonances (Morbidelli and Moons, 1995). A brief account of this new development is given in section 4.

The 2:1 MMR with Jupiter at 3.27 AU is a unique case, because here the chaotic secular resonances are located at high eccentricities (Morbidelli and Moons, 1993). Yet in the early 1990s, only a few asteroids were known to exist on resonant orbits, in contrast to the large nonresonant populations on either side of the 2:1 MMR. The studies devoted to the question of the long-term stability of the resonant orbits were marked by the evolution of the numerical methods (Wisdom and Holman, 1991; Levison and Duncan, 1994) and the computer speed. Important progress was made when the globally chaotic nature of orbits in the 2:1 MMR was demonstrated (Ferraz-Mello, 1994b). Later works (Morbidelli, 1996; Nesvorný and Ferraz-Mello, 1997; Ferraz-Mello et al., 1998a) showed that this resonance is an intermediate case between the unstable MMRs and stable 3:2 MMR with Jupiter, the latter hosting the Hilda group. The 2:1 MMR possesses a core with dynamical lifetime comparable to the age of the solar system, where currently nearly 30 small asteroids are known (the Zhongguo group). We devote section 5 to this subject.

A major breakthrough, already signaled by the studies of the slow chaos in the 2:1 MMR, was made concerning

the phenomenon referred to as “stable chaos.” It was previously noted that a large number of asteroids have strongly chaotic orbits yet are stable on long intervals of time (*Milani and Nobili, 1992; Milani et al., 1997*). The main reason for such behavior was revealed by the discovery of the so-called three-body resonances, i.e., MMRs, where the commensurability of orbital periods occurs between an asteroid and two planets [mainly Jupiter and Saturn; (*Murray et al., 1998, Nesvorný and Morbidelli, 1998*)]. The subsequent modeling of these resonances showed that they represent narrow but strongly chaotic layers densely intersecting the asteroid belt (section 6.1).

The slow chaotic evolution observed in numerical simulations in the narrow MMRs in the outer asteroid belt was explored by *Murray and Holman (1997)*. This study correctly showed that the mechanism driving the chaotic diffusion lies in the “multiplet structure” of the narrow MMRs (section 6.2).

The study of the dynamics in the inner belt (2.1–2.5 AU) revealed surprising instabilities of asteroid orbits. Numerical simulations showed that many asteroids currently on non-planet-crossing orbits with large eccentricities evolve to Mars-crossing orbits within the next 100 m.y. (*Migliorini et al., 1998, Morbidelli and Nesvorný, 1999*). The responsible resonances in this case are the MMRs with Mars, previously thought unimportant because of the small mass of this planet. The MMRs with Mars were identified as a major source of the large near-Earth asteroids (NEAs; section 6.3). They were also conjectured to disperse the asteroid families in the inner asteroid belt (*Nesvorný et al., 2002*).

After introducing basic notation (section 2) and showing the global structure of MMRs in the asteroid belt (section 3), we follow the above historical overview. Section 2 is directed toward the reader who wishes to gain some basic insight in the mathematical methods developed and utilized in studies of MMRs. Perspectives are given in the last section.

## 2. NOTATION AND BASIC TERMINOLOGY

A mean-motion resonance (MMR) occurs when an asteroid has an orbital period commensurate with the orbital period of one or more of the planets. To fix the notation, we define

$$\sigma_{\mathbf{k},\mathbf{l},\mathbf{m}} = \sum_{j=1}^N k_j \lambda_j + k\lambda + \sum_{j=1}^N l_j \bar{\omega}_j + l\bar{\omega} + \sum_{j=1}^N m_j \Omega_j + m\Omega \quad (1)$$

where  $\mathbf{k}$ ,  $\mathbf{l}$ ,  $\mathbf{m}$  and  $\mathbf{k} = (k_1, \dots, k_N)$ ,  $\mathbf{l} = (l_1, \dots, l_N)$ ,  $\mathbf{m} = (m_1, \dots, m_N)$  are integers with zero sum:  $k + l + m + \sum(k_j + l_j + m_j) = 0$  (because of the invariance of interaction by rotation, only such combinations exist; this and other conditions on integer coefficients required by symmetries of the gravitational interaction are known as D’Alembert rules), and  $k \neq 0$  and  $\|\mathbf{k}\| \neq 0$  (i.e., MMRs are related to the fast orbital frequencies, unlike the secular resonances). Here  $\lambda$ ,

$\bar{\omega}$ ,  $\Omega$ ,  $\lambda_j$ ,  $\bar{\omega}_j$ ,  $\Omega_j$  are orbital angles in the usual notation (index  $j$  goes over  $N$  planets).

The MMR occurs when  $\dot{\sigma}_{\mathbf{k},\mathbf{l},\mathbf{m}} = 0$ , where  $\dot{\sigma}_{\mathbf{k},\mathbf{l},\mathbf{m}}$  is the time derivative of  $\sigma_{\mathbf{k},\mathbf{l},\mathbf{m}}$  given by equation (1). In the case of asteroid motion, the secular frequencies  $\bar{\omega}$ ,  $\bar{\omega}_j$ ,  $\Omega$ ,  $\Omega_j$  are small compared to the orbital frequencies  $\lambda$ ,  $\lambda_j$ . For this reason,  $\dot{\sigma}_{\mathbf{k},\mathbf{l},\mathbf{m}} = 0$  is approximately  $\sum k_j \lambda_j + k\lambda = 0$ , which can be solved for the resonant semimajor axis ( $a_{\text{res}}$ ) in the Keplerian approximation. This means that resonant conditions  $\dot{\sigma}_{\mathbf{k},\mathbf{l},\mathbf{m}} = 0$  with unique  $\mathbf{k}, \mathbf{l}$  but different  $\mathbf{l}, \mathbf{m}$  hold at about the same semimajor axis. Thus, each  $(\mathbf{k}, \mathbf{l})$  MMR may be thought to be composed from several resonant terms with different  $\mathbf{l}, \mathbf{m}$  (this structure is called the “resonant multiplet”).

In practice, there are two important cases: (1) the two-body MMR, when index  $\mathbf{k}$  has only one nonzero integer  $k_{j_1}$  where  $j_1$  denotes, in the asteroid belt, either Jupiter or Mars (a few two-body resonances with Saturn and the Earth occur but they are of minor importance), and (2) the three-body MMR, when index  $\mathbf{k}$  has two nonzero integers,  $k_{j_1}$  and  $k_{j_2}$ , corresponding to two planets (mainly to pairs Jupiter–Saturn and Mars–Jupiter). Without loss of generality we assume that  $k_{j_1} > 0$ .

The notation of MMRs that we adopt in the following text is that a  $(\mathbf{k}, \mathbf{l})$  two-body MMR with Jupiter ( $j_1 = 5$ ) is  $k_5 J: -k$ , and with Mars ( $j_1 = 4$ ) is  $k_4 M: -k$ , where  $k_4$ ,  $k_5$ , and  $k$  are integers defining the resonant angle in equation (1). In this notation, 2J:1 is a MMR with Jupiter, where an asteroid has the orbital period of one-half that of Jupiter. Moreover, if it is clear from the text which planet is considered, we drop the letter indicating the planet (2J:1 becomes 2:1 as frequently used in the literature). Concerning the three-body resonances we denote  $k_5 J: k_6 S: k$  for the MMRs with Jupiter and Saturn, and  $k_4 M: k_5 J: k$  for the MMRs with Mars and Jupiter. (This notation attempts to generalize the classical notation, i.e., the minus sign in  $k_{j_1}: -k$  for two-body MMRs, to the case of three-body MMRs and MMRs with planets other than Jupiter.)

The equations of motion of an asteroid in the presence of a MMR can be conveniently written in the Hamiltonian formalism. In such formalism, the equations of motion derive from a function of the canonical variables (the Hamiltonian). This formulation is useful because it allows us to use rigorous methods for treating problems where an integrable system is coupled with small perturbations (in the current context, the asteroid’s motion about the Sun is perturbed by the planets).

The classical expression for the Hamiltonian of a small body evolving under the gravitational force of the Sun and  $N$  planets is

$$\mathcal{H} = -\frac{1}{2a} - \sum_{j=1}^N \mu_j \mathcal{R}_j \quad (2)$$

$$\mathcal{R}_j = \frac{1}{\Delta_j} - \frac{\mathbf{r} \cdot \mathbf{r}_j}{r_j^3}$$

where  $\Delta_j = |\mathbf{r} - \mathbf{r}_j|$  and  $\mathbf{r}, \mathbf{r}_j$  are the heliocentric positions of

the small body and planet  $j$  respectively, and  $a$  is the semi-major axis of the small body. (We adopt units where the product of the gravitational constant and the mass of the Sun is 1.) Here,  $1/2a$  is the heliocentric Keplerian part and  $\mu_j \mathcal{R}_j$  is the perturbation exerted by the planet  $j$  having mass  $\mu_j$ .

Appropriate canonical variables of the Hamiltonian equation (2) are the so-called modified Delaunay variables

$$\begin{aligned} \lambda & & \Lambda &= L \\ p &= -\varpi & P &= L - G \\ q &= -\Omega & Q &= G - H \end{aligned} \quad (3)$$

where  $L = \sqrt{a}$ ,  $G = L\sqrt{1 - e^2}$  and  $H = G \cos i$  are the usual Delaunay variables ( $e$  and  $i$  are the eccentricity and inclination of the small body respectively). The perturbation  $\mathcal{R}_j$  can be written as a function of the orbital elements of the small body and planet  $j$  [see *Moons* (1993) for such an expression with general validity]. The Hamiltonian equation (2) is then expressed in terms of variables defined in equation (3).

To realistically account for the motion of the planets, the time evolution of the planetary orbital elements, provided by the planetary theory (*Laskar, 1988; Bretagnon and Simon, 1990*), must be substituted in  $\mathcal{R}_j$ . If we denote the planetary orbital elements by index  $o$  (as osculating) to distinguish them from the proper orbital elements (the latter being denoted by  $a_j, e_j, i_j, \lambda_j, \varpi_j, \Omega_j$ ), the general form of the quasi-periodic evolution of the planetary elements is

$$\begin{aligned} a_j^o &= a_j + \sum_v A_v \cos \Psi_v \\ \lambda_j^o &= \lambda_j + \sum_v B_v \cos \Psi_v \\ e_j^o \exp i\varpi_j^o &= e_j \exp i\varpi_j + \sum_v C_v \cos \Psi_v \\ i_j^o \exp i\Omega_j^o &= i_j \exp i\Omega_j + \sum_v D_v \cos \Psi_v \end{aligned} \quad (4)$$

where  $\Psi_v = \sum_j (r_j \lambda_j + s_j \varpi_j + t_j \Omega_j)$ , the multiindex  $v$  denoting different values of integers  $r_j, s_j, t_j$ , and  $i = \sqrt{-1}$ .

By definition, the proper angles evolve linearly with time, with fixed frequencies provided by the planetary theory. We will denote by  $n_j, g_j, s_j$  the orbital, perihelion, and node frequencies respectively. In fact, because  $A_v, B_v, C_v, D_v$  in equation (4) are small, the new  $\mathcal{R}_j$  — functions of the planetary proper elements — are at the first approximation identical to the original functions. There will, however, appear important terms at second and higher orders in the planetary masses generated by the substitution of equation (4) in equation (2). A number of approximations of equation (4) are used in the literature, varying from the planar model with one planet on the circular orbit [ $a_j^o = a_j, \lambda_j^o = \lambda_j = n_j t, e_j = i_j = 0$ , where  $n_j = \sqrt{(1 + \mu_j)/a_j^3}$  and  $t$  is time] to more realistic ones.

To summarize, it is understood at this point that although we do not explicitly show such an expression, the Hamiltonian equation (2) is a function of equation (3) and the planets' proper elements (through the substitution in equa-

tion (4)). This is an autonomous Hamiltonian of  $3(N + 1)$  degrees of freedom with the general form

$$\mathcal{H} = \mathcal{H}_0 + \mu \mathcal{H}_1 + \mu^2 \mathcal{H}_2 + \mathcal{O}(\mu^3) \quad (5)$$

where

$$\mathcal{H}_0 = -\frac{1}{2\Lambda^2} + \sum_{j=1}^N (n_j \Lambda_j + g_j \Lambda_{g_j} + s_j \Lambda_{s_j}) \quad (6)$$

Here,  $\mu$  denotes the largest of the masses of the involved planets, and  $\Lambda_j, \Lambda_{g_j}, \Lambda_{s_j}$  are the canonical momenta conjugate to the proper angles  $\lambda_j, \varpi_j, \Omega_j$ .

To first order in  $\mu$ , the elimination of the fast orbital angles by the Lie-series canonical transformation (see, e.g., *Hori, 1966*) is equivalent to averaging equation (5) over  $\lambda_j, j = 1, \dots, N$ , maintaining only the terms in which  $\lambda, \lambda_{j_1}, \lambda_{j_2}$  appear in resonant combinations  $\sigma_{\mathbf{k}, \mathbf{k}, \mathbf{l}, \mathbf{l}, \mathbf{m}, \mathbf{m}}$  [corresponding to the  $(\mathbf{k}, \mathbf{k})$  MMR in question]. This procedure is straightforward if one utilizes the resonant variables in equation (5)

$$\sigma = \frac{k_{j_1} \lambda_{j_1} + k_{j_2} \lambda_{j_2} + k\lambda + (k_{j_1} + k_{j_2} + k)p}{k_{j_1} + k_{j_2} + k} \quad S = P$$

$$v = -\frac{k_{j_1} \lambda_{j_1} + k_{j_2} \lambda_{j_2} + k\lambda}{k_{j_1} + k_{j_2} + k} \quad N = \frac{k_{j_1} + k_{j_2} + k}{k} \Lambda + P + Q$$

$$\sigma_z = \frac{k_{j_1} \lambda_{j_1} + k_{j_2} \lambda_{j_2} + k\lambda + (k_{j_1} + k_{j_2} + k)q}{k_{j_1} + k_{j_2} + k} \quad S_z = Q$$

$$\lambda_{j_1} \quad \tilde{\Lambda}_{j_1} = \Lambda_{j_1} - \frac{k_{j_1}}{k} \Lambda$$

$$\lambda_{j_2} \quad \tilde{\Lambda}_{j_2} = \Lambda_{j_2} - \frac{k_{j_2}}{k} \Lambda$$

$$\lambda_j, j \neq j_1, j_2 \quad \Lambda_j, j \neq j_1, j_2 \quad (7)$$

where, in the case of a two-body MMR with the  $j_1$ -th planet,  $k_{j_2} = 0$ . The Hamiltonian equation (2) written in canonical variables defined by equation (7) is then simply averaged over  $\lambda_j, j = 1, \dots, N$ . The resulting Hamiltonian of the two-body MMR is

$$\begin{aligned} \mathcal{H}^{2\text{BR}} &= -\frac{1}{2\Lambda^2} + \frac{k_{j_1}}{k} n_{j_1} \Lambda + \sum_{j=1}^N (g_j \Lambda_{g_j} + s_j \Lambda_{s_j}) + \\ &\mu \bar{\mathcal{H}}_1(S, N, S_z, \sigma, v, \sigma_z, \varpi, \Omega) + \mathcal{O}(\mu^2) \end{aligned} \quad (8)$$

where

$$\mu \bar{\mathcal{H}}_1 = -\frac{1}{2\pi} \sum_{j=1}^N \mu_j \int_0^{2\pi} \mathcal{R}_j d\lambda_j \quad (9)$$

and  $\varpi = (\varpi_1, \dots, \varpi_N), \Omega = (\Omega_1, \dots, \Omega_N)$ .

In the case of a three-body MMR,  $\bar{\mathcal{H}}_1$  in equation (9) contains only terms dependent on  $\varpi = -\sigma - v$  and/or  $\Omega = -\sigma_z - v$ ,

because  $\mathcal{R}_j$  depends solely on the variables of the small body and  $j$ -th planet. The resonant terms of three-body MMRs appear at second- and higher-order terms in  $\mu$ . These terms are generated by the substitution of the planetary orbital elements (equation (4)) (the so-called “indirect” contribution) and by iterating the Lie-series transformation elimination of fast orbital angles to higher orders in  $\mu$  (the so-called “direct” contribution). This procedure was described in *Nesvorný and Morbidelli* (1999). The resonant Hamiltonian of the three-body MMR is

$$\begin{aligned} \mathcal{H}^{3BR} = & -\frac{1}{2\Lambda^2} + \frac{k_{j_1}n_{j_1} + k_{j_2}n_{j_2}}{k} \Lambda + \\ & \sum_{j=1}^N (g_j \Lambda_{g_j} + s_j \Lambda_{s_j}) + \\ & \mu \bar{\mathcal{H}}_1(S, N, S_z, \sigma + v, \sigma_z + v, \bar{\omega}, \Omega) + \\ & \mu^2 \bar{\mathcal{H}}_2(S, N, S_z, \sigma, v, \sigma_z, \bar{\omega}, \Omega) + \mathcal{O}(\mu^3) \end{aligned} \quad (10)$$

Note that equations (8) and (10) have  $2N + 3$  degrees of freedom (i.e.,  $N$  less than equation (5)).

Thus, we learn an important difference between the two- and three-body MMRs, which is that the magnitudes of the resonant terms are proportional to the planetary mass and to the planetary mass squared respectively. As the planetary masses in our solar system are  $<10^{-3}$  (in solar units), this shows that a typical two-body MMR is expected to have a larger effect on an asteroid’s orbit than a typical three-body MMR would have. To document this fact, let us consider an Hamiltonian with only one  $\sigma_{\mathbf{k},\mathbf{k},\mathbf{l},\mathbf{l},\mathbf{m},\mathbf{m}}$  (i.e., fixing  $\mathbf{k},\mathbf{k},\mathbf{l},\mathbf{l},\mathbf{m},\mathbf{m}$ , and ignoring terms in equations (8) and (10) with other than this multiindex). Such a Hamiltonian accounts for a single isolated multiplet term of the  $(\mathbf{k},\mathbf{k})$  MMR. The phase portrait of trajectories of a single multiplet term is basically equivalent to the phase portrait of trajectories of a pendulum. The width in semimajor axis, represented by the maximal extent of the pendulum separatrixes, is

$$\Delta a = 8a_{\text{res}}^{3/2} \sqrt{\frac{\beta}{3}} \quad (11)$$

where  $\beta$  is the coefficient in front of the cosine of the specific multiplet term in the Fourier expansion of the resonant parts in equations (8) and (10) (*Murray et al.*, 1998; *Nesvorný and Morbidelli*, 1999). In the case of the two-body MMR, this coefficient is  $\propto \mu_{j_1} P(e, e_{j_1}, i, i_{j_1})$ , where  $P$  is a polynomial in  $e, e_{j_1}, i, i_{j_1}$  with the total power of each term being at least  $\rho = |k_{j_1} + k|$  (called the resonant order). From equation (11), the width of the two-body resonance is then  $\propto \sqrt{\mu_{j_1}} a_{\text{res}}^{3/2} P^{1/2}$ . For the three-body MMR,  $\rho = |k_{j_1} + k_{j_2} + k|$  and its width is  $\propto \mu a_{\text{res}}^{3/2} P^{1/2}$ . Consequently, the two-body MMR is generally larger than the three-body MMR due to the mass factor. On the other hand, there are typically more three-body MMRs than two-body MMRs within a semima-

ior axis interval, because three integers ( $k_{j_1}, k_{j_2}, k$ ) allow for a larger number of combinations than two integers ( $k_{j_1}, k$ ). In some sense, the larger density of three-body MMRs in the orbital space compensates for their smaller widths, so that both two- and three-body MMRs are important for asteroid dynamics.

### 3. OVERLAPPING MEAN-MOTION RESONANCES AND THE GLOBAL STRUCTURE OF THE ASTEROID BELT

Let us consider the two-body resonances only. Figure 1 shows the structure of resonant trajectories for the 3J:2 (Figs. 1a,b), 3J:1 (Fig. 1c), 5J:2 (Fig. 1d) and 5M:9 (Figs. 1e,f). The model used for the Jupiter’s MMRs (Figs. 1a–d) is an approximation of equation (8) assuming coplanar orbits and a circular orbit for Jupiter. In such case the first-order resonant Hamiltonian is

$$\begin{aligned} \mathcal{H}^{\text{PC}} = & -\frac{k_5^2}{2k^2} (N - S)^{-2} + \\ & n_5 (N - S) + \mu_5 \bar{\mathcal{H}}_1(S, N, \sigma) \end{aligned} \quad (12)$$

It does not depend on  $S_z, \sigma_z$  because of the coplanarity, and does not depend on  $v$  because  $\mathcal{R}_5$  in equation (2) is invariant by rotation around an axis perpendicular to the orbital plane. Consequently,

$$N = \sqrt{a} \left[ 1 - \sqrt{1 - e^2} + \frac{k_5 + k}{k} \right] = \text{const}$$

and trajectories can be obtained as level curves of the Hamiltonian in equation (12).

In Fig. 1, two  $N = \text{const}$  manifolds are shown for the 3J:2 (first-order MMR,  $a_{\text{res}} = 3.97$  AU) corresponding to eccentricities under (Fig. 1a) and above (Fig. 1b) the Jupiter-crossing limit. The Jupiter-crossing limit is  $e \approx 0.31$ . Resonant orbits with  $e \geq 0.31$  may intersect the orbit of Jupiter. The bold line in Fig. 1b is where collisions take place. There are two equilibria in Fig. 1a: the stable one at  $\sigma = 0$  (libration center) and the unstable one at  $\sigma = \pi$ . The trajectories connected to the unstable equilibrium are called separatrixes. The trajectories enclosing the stable equilibrium are the resonant ones. They are characterized by oscillations of  $\sigma$  about 0 (so-called “libration”). Above the Jupiter-crossing limit (Fig. 1b), the trajectories near the libration center are protected from collisions. This happens due to the so-called “resonant phase-protection mechanism,” which guarantees that conjunctions with Jupiter occur when the resonant asteroid is near the perihelion of its orbit, i.e., far from Jupiter.

The 3J:1 MMR (second order) has two libration centers at  $\pi/2$  and  $3\pi/2$  (Fig. 1c) and occurs closer to the Sun ( $a_{\text{res}} = 2.5$  AU), where collisions with Jupiter cannot happen on elliptic heliocentric orbits. The 5J:2 MMR (third order) has, in addition to the libration center at 0, two other centers at  $2\pi/3$  and  $4\pi/3$  (Fig. 1d). In general, the two-body MMRs interior of the planet’s orbit ( $|k_{j_1}| > |k|$ ) have libration cen-

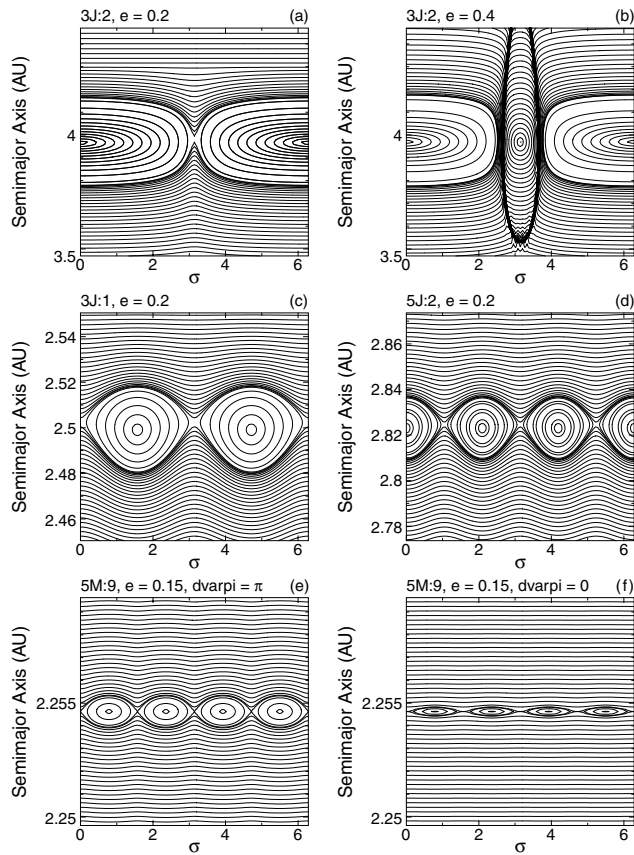


**Fig. 1.** Trajectories at MMRs. (a,b) 3J:2 below (a) and above (b) the Jupiter-crossing limit; (c) 3J:1 MMR; (d) 5J:2 MMR; (e,f) 5M:9 MMR with  $\varpi - \varpi_4 = \pi$  (e) and  $\varpi - \varpi_4 = 0$  (f). On x-axis,  $\sigma$  is defined by equation (7).

ters at  $\sigma_c = 2j_1\pi/\rho$  if  $\rho$  is odd and at  $\sigma_c = (2j_1 + 1)\pi/\rho$  if  $\rho$  is even. The exterior resonances have the libration centers at  $\sigma_c = (2j_1 + 1)\pi/\rho$  if  $k_{j_1} \neq 1$ . Conversely, if  $k_{j_1} = 1$ , the structure of the exterior resonance is characterized by so-called asymmetric librations where none of the  $2\rho$  libration centers is at  $2j_1\pi/\rho$  or  $(2j_1 + 1)\pi/\rho$  for most values of  $N$  (Message, 1958; Beaugé, 1994).

An interesting case is that of the two-body MMRs with Mars, due to the large modulation of their widths with the evolution of perihelion longitudes and eccentricities. Figures 1e and 1f show the trajectories near the 5M:9 MMR ( $a_{\text{res}} = 2.253$  AU) in the coplanar model with Mars on a fixed elliptic orbit ( $e_4 = 0.065$ ), assuming two values of perihelion longitudes:  $\varpi - \varpi_4 = \pi$  in Fig. 1e and  $\varpi - \varpi_4 = 0$  in Fig. 1f. In general, when  $\varpi - \varpi_{j_1} = \pi$ , the MMRs have their maximum widths. For other phases of the secular angles, the sizes of resonant islands are smaller.

The resonant width (i.e., the width of the libration island) can be conveniently estimated by measuring the distance between separatrices for  $\sigma = 0$  (for interior resonances of odd order) or  $\sigma = \pi/\rho$  (for interior resonances of even order and exterior resonances with  $k_j \neq 1$ ). For the exterior reso-

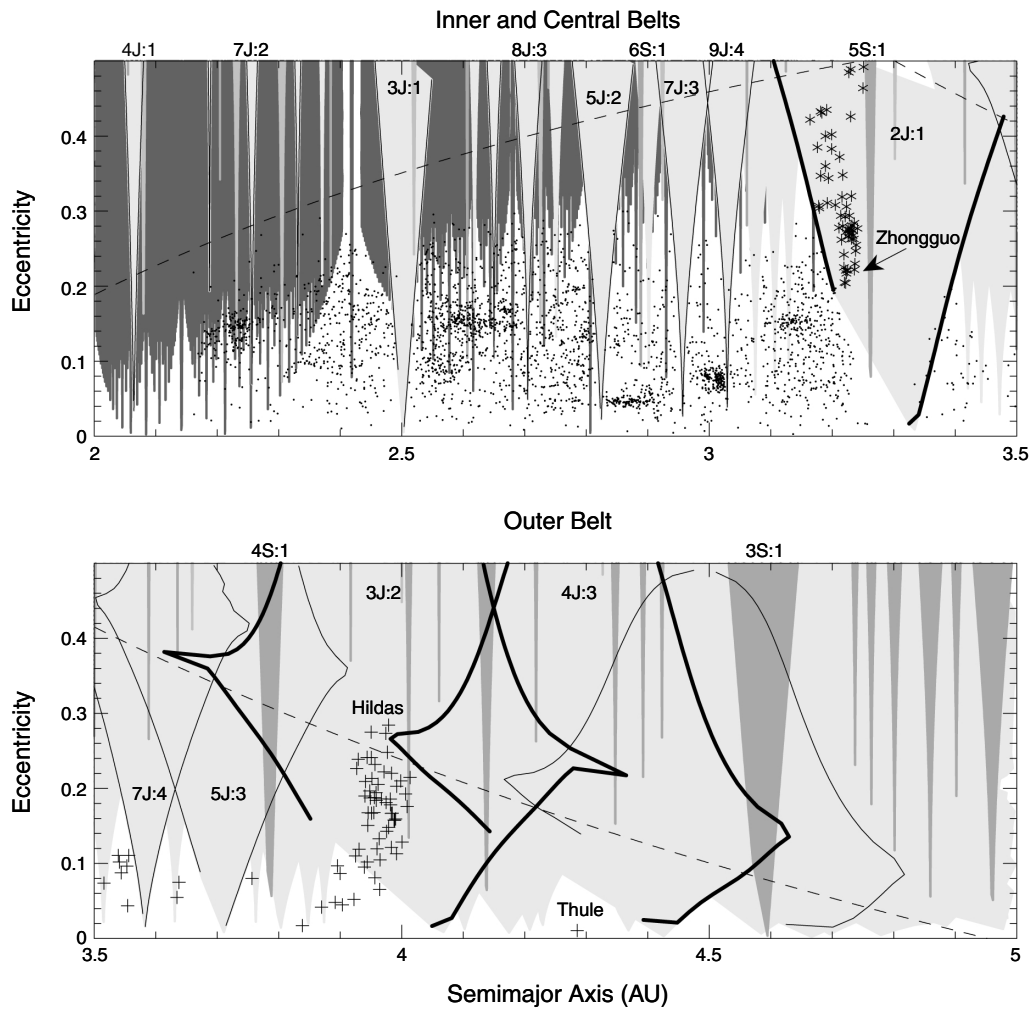
nances with  $k_j = 1$ , the separatrix distance is measured at  $\sigma_c$ , which must be determined beforehand as an extreme of equation (12). Iterating the algorithm over levels of  $N = \text{const}$ , the resonant width  $\Delta a$  can be determined as a function of  $e$ .

Figure 2 shows the MMRs in the asteroid belt. It is an extension of a similar result obtained by Dermott and Murray (1983), but accounting for all MMRs with  $\Delta a > 10^{-4}$  AU. We also plot in this figure the asteroids with magnitudes up to the current level of completeness (Jedicke and Metcalfe, 1998). The orbital distribution of these bodies is thus unaffected by observational biases. In the region of the 2J:1, the resonant orbital elements of all known resonant objects, regardless of size, are shown.

To correctly interpret this figure, one should be aware of the now-classical result of Chirikov (1979) known as the “resonance overlap criterion.” This criterion affirms that whenever two resonances with similar sizes overlap, the corresponding resonant orbits become chaotic. The same criterion was used by Wisdom (1980) to show the onset of chaos in the vicinity of a planet because of the overlap of the first-order MMRs with Jupiter. This criterion can be used in the current context to explain why there are so few asteroids located above the threshold in  $e$  for the resonance overlap. Moreover, we know from the experience obtained in the last few years with the secular dynamics inside the MMRs that MMRs themselves are usually characterized by chaotic dynamics (see next section). In resonances like the 3J:1 and 5J:2 MMRs (at 2.5 and 2.82 AU), and many others, the chaos causes large-scale instabilities: The resonant bodies evolve to high- $e$  orbits and are removed from resonant orbits by encounters with Mars or Jupiter (Gladman et al., 1997). Such resonances are associated with the Kirkwood gaps in the asteroid distribution. Smaller MMRs, albeit strongly chaotic, do not generate strong instabilities whenever eccentricities are not near a planet-crossing limit. Large first-order MMRs are characterized by either marginal instabilities (like 2J:1 at 3.27 AU) or possess cores in which orbital lifetimes exceed the solar system age (such as the 3J:2 MMR at 3.97 AU and the low- $e$  region in the 4J:3 MMR at 4.29 AU, where 279 Thule is located).

The basic impression one has from Fig. 2 is that the MMRs delimit the orbital space inhabited by the observed asteroids in  $a$  and  $e$ . Due to chaos and instabilities generated by MMRs, this is quite intuitive. Most of the job in removing the material from the belt was apparently done by several large MMRs with Jupiter (as 3J:1, 5J:2, 7J:3, 9J:4, 7J:4, 5J:3, etc.) and many narrow MMRs with Mars. It is not more than a curiosity that a few MMRs with Saturn and Earth also exist in the inner and central asteroid belts (6S:1 at 2.89 AU, 7S:1 at 2.61 AU, 2E:7 at 2.305 AU, 2E:9 at 2.73 AU, etc.).

We have accounted solely for two-body MMRs in Fig. 2. This happens to be a good approximation when considering the gross structures of the asteroid belt in  $a$  and  $e$ , but becomes less acceptable when one’s objective is to under-



**Fig. 2.** Global structure of the MMRs in the asteroid belt. There are four different gray shades denoting the regions of resonant motion with planets: light gray for Jupiter MMRs, intermediate for Saturn MMRs, and dark gray for Mars MMRs. Each resonance corresponds to one V-shaped region except the large first-order MMRs with Jupiter, which have particular shapes. Some of the resonances are labeled. For some Jupiter MMRs the projection of separatrixes on the  $a, e$  plane is shown by black lines; for 2J:1, 3J:2, and 4J:3, these lines are bold. We also show the proper (dots; *Milani and Knežević*, 1994) or orbital elements (crosses; *Bowell et al.*, 1994) of asteroids with magnitudes up to the completeness level. In case of the group of small asteroids in the 2J:1 MMR (arrow indicates 3789 Zhongguo), the resonant elements are plotted (asterisks; *Roig et al.*, 2002). Other resonant asteroids are the Hilda group in the 3J:2 MMR and 279 Thule in the 4J:3 MMR. The orbits above the dashed lines are planet-crossing.

stand the dynamics of real bodies. The three-body resonances are usually as narrow as two-body resonances with Mars ( $<10^{-2}$  AU), but generally being of a low order, they have nonnegligible sizes down to small eccentricities. Moreover, the three-body MMRs are numerous.

#### 4. CHAOTIC SECULAR DYNAMICS IN THE MEAN-MOTION RESONANCES WITH JUPITER: THE KIRKWOOD GAPS

The bodies inside the wide MMRs with Jupiter undergo important secular dynamics, in particular for what concerns the evolution of  $e$  (*Wisdom*, 1982; *Yoshikawa*, 1990, 1991;

*Ferraz-Mello and Klafke*, 1991; *Morbidelli and Moons*, 1995; *Gladman et al.*, 1997). We briefly review how this can be theoretically justified, restricting for simplicity to the case where the asteroid and planets have coplanar orbits, although elliptic and precessing [see *Morbidelli and Moons* (1993) for a discussion of the inclined case]. We start from the resonant Hamiltonian equation (8), that we rewrite as  $\mathcal{H}^{2BR} = \mathcal{H}^{PC} + \mathcal{F}$  where  $\mathcal{H}^{PC}$  is given in equation (12), and  $\mathcal{F} = \mathcal{H}^{2BR} - \mathcal{H}^{PC}$ . The function  $\mathcal{F}$  can be considered as a perturbation of  $\mathcal{H}^{PC}$ , because (for D'Alembert rules) the former is proportional to the planetary eccentricities.

Because  $\mathcal{H}^{PC}$  is integrable, we introduce the Arnold action-angle variables in the MMR region where  $\sigma$  librates.

Following *Henrard (1990)*, the transformation has the form

$$\begin{aligned} \psi_\sigma &= \frac{2\pi}{T_\sigma} t & J_\sigma &= \frac{1}{2\pi} \oint S \, d\sigma \\ \psi_\nu &= \nu - f(\psi_\sigma, J_\sigma, J_\nu) & J_\nu &= N \end{aligned} \tag{13}$$

where the integral is done over a trajectory of  $S$ ,  $\sigma$  for  $N = \text{const}$  (Fig. 1),  $T_\sigma$  is a period of the trajectory, and  $f$  is a periodic function of  $\psi_\sigma$ , with null average.

We then write  $\mathcal{H}^{\text{PC}}$  and  $\mathcal{F}$  as functions of these variables. By construction,  $\mathcal{H}^{\text{PC}}$  now depends only on the new action variables  $J_\sigma$ ,  $J_\nu$ . By averaging  $\mathcal{F}$  over  $\psi_\sigma$ , we obtain an Hamiltonian of the form

$$\mathcal{H}^{\text{SEC}} = \sum_j g_j \Lambda_{g_j} + \mathcal{H}^{\text{PC}}(J_\sigma, J_\nu) + \bar{\mathcal{F}}(J_\sigma, J_\nu, \psi_\nu, \varpi) \tag{14}$$

where  $\varpi = (\varpi_1, \dots, \varpi_N)$ . Because this Hamiltonian is inde-

pendent of  $\psi_\sigma$ , the action  $J_\sigma$  is now a constant of motion. Thus, equation (14) describes the secular dynamics inside the MMR, namely the evolution of the eccentricity (through  $J_\nu$ ) due to the motion of the perihelia of the asteroid and the planets ( $-\nu$  and  $\varpi_j$  respectively).

The mean frequency of the longitude of perihelion can be computed as

$$-\dot{\psi}_\nu = \frac{\partial \mathcal{H}^{\text{SEC}}}{\partial J_\nu} \tag{15}$$

A first-order perihelion secular resonance occurs when  $\dot{\psi}_\nu + g_j = 0$ , where  $g_j$  is the frequency of  $\varpi_j$  [for numeric values of  $g_j$  see, e.g., *Laskar (1988)*].

It often occurs in MMRs with Jupiter that the secular resonances associated with the  $g_5$  and  $g_6$  frequencies are located close to each other. To study the effects of the interaction between these two resonances, we construct a two-resonance model by retaining from equation (14) the har-

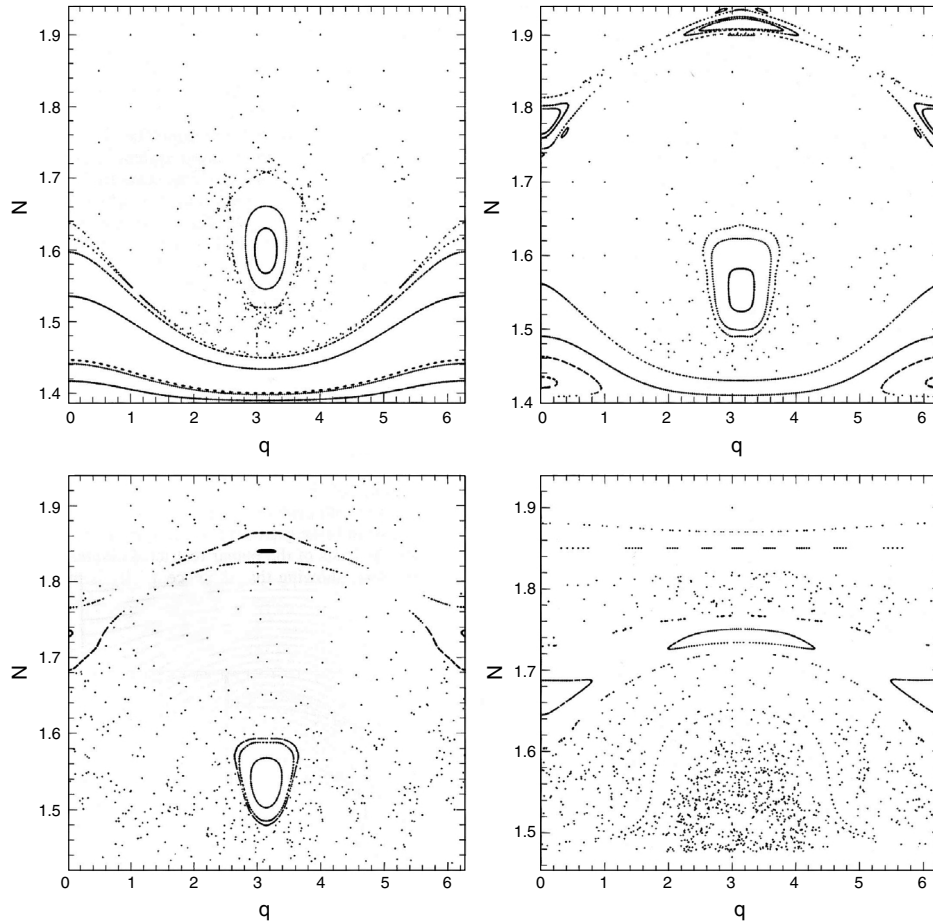


**Fig. 3.** Sections of the dynamics of equation (16) computed at  $\sigma_6 = 0$  for the 3J:1 MMR. The four panels correspond to increasing values of  $J_\sigma$ , the latter being related to the amplitude of oscillation of  $a$ . The label  $q$  stands for  $\varpi - \varpi_5$ , while  $N = J_\nu = \sqrt{a(3 - \sqrt{1 - e^2})}$ . At the center of the 3J:1, the values  $N = 1.4, 1.5, 1.6, 1.7, 1.8, 1.9$  correspond to  $e = 0.2, 0.55, 0.72, 0.84, 0.92, 0.97$  respectively. In each panel, the lower limit on the  $N$  axis is the value that identifies the separatrix of the MMR. Consequently, all the curves that seem to exit from the bottom border of the panels correspond to trajectories that hit the separatrix of the MMR during their secular evolution, and are therefore expected to be chaotic. From *Moons and Morbidelli (1995)*.

monic of  $\bar{\mathcal{F}}$  with arguments  $\sigma_5 = \psi_v + \bar{\omega}_5$  and/or  $\sigma_6 = \psi_v + \bar{\omega}_6$ . Thus, we consider the Hamiltonian

$$\begin{aligned} \mathcal{H}^{5,6} = & g_5 \Lambda_{g_5} + g_6 \Lambda_{g_6} + \\ & \mathcal{H}^{\text{PC}}(J_\sigma, J_v) + \bar{\mathcal{F}}^{5,6}(J_\sigma, J_v, \sigma_5, \sigma_6) \end{aligned} \quad (16)$$

This is a nonintegrable Hamiltonian that must be studied numerically. The dynamics can be represented on the  $\sigma_5, J_v$  plane, for instance through a section at  $\sigma_6 = 0$ . The sections depend parametrically on  $J_\sigma$ , roughly corresponding to the libration amplitude of a ( $A_a$ ).

In the case of the 3:1 MMR with Jupiter (Fig. 3), most of the phase space is covered by a chaotic region, which extends up to  $e = 1$  (top borders of the panels). Only the orbits with small  $A_a$  and  $e$  (the smooth curves at the bottom of the two top panels of Fig. 3) still have regular dynamics. These orbits, however, periodically reach Mars-crossing eccentricities ( $e > 0.3$ ); the encounters with Mars give impulsive changes to  $a$  and  $e$ , which, although generally very small, effectively modify  $A_a$ . At large  $A_a$ , the chaotic region generated by the overlap of the  $v_5$  and  $v_6$  resonances extends to all eccentricities (bottom panels of Fig. 3), and the asteroid can therefore rapidly and chaotically evolve to very large  $e$ . This combination of large-scale chaos of the secular dynamics and weak martian encounters explains the behavior of 3:1 resonant asteroids observed in numerical integrations of the full equations of motion (see *Morbidelli et al.*, 2002), and explains the formation of a gap in the asteroid distribution.

The same happens in many other major MMRs with Jupiter that are associated with a Kirkwood gap. *Moons and Morbidelli* (1995) have shown that also the 4J:1, 5J:2, and 7J:3 MMRs are dominated by the chaotic region generated by the overlap of the  $v_5$  and  $v_6$  resonances, so that the asteroids in these MMRs can also reach very large  $e$  on a timescale of a few million years.

Large evolutions of  $e$  in many MMRs are typically caused by the secular resonance  $v_5$  itself. The structure of the  $v_5$  resonance can be computed in models neglecting  $g_6$  (*Ferraz-Mello and Klafke*, 1991; *Klafke et al.*, 1992; *Moons and Morbidelli*, 1995). These models show that by the effect of  $v_5$ , the eccentricity suffers large variations, while  $\bar{\omega} - \bar{\omega}_5$  oscillates around 0 or  $\pi$ . In such models, however, only bodies with certain initial orbits can evolve from low to very high eccentricities (*Klafke et al.*, 1992). Other parts of the orbital space are characterized by regular motion bounded at moderate  $e$ . This regular motion almost completely vanishes when  $g_6$  is accounted for (as shown above; Fig. 3). Consequently, in a globally chaotic environment, orbits evolve according to the underlying structure of  $v_5$ , and despite their initial location in the orbital space, reach very large  $e$ . This is usually accomplished by a series of small transitions because of the interaction of  $v_5$  and  $v_6$  and a few large events, when  $e$  increases due to the effect of  $v_5$  (*Morbidelli and Moons*, 1995).

## 5. TRANSIENT AND STABLE POPULATIONS OF THE 2J:1 AND 3J:2 MEAN-MOTION RESONANCES

In the 2J:1 and 3J:2 MMRs, simple models with Jupiter's orbit fixed also show a high- $e$  regime of motion associated with the  $v_5$  resonance. In this case, however, the high- $e$  regime is separated from low  $e$  by regular orbits, which are robust and persist in the models that account for  $g_6$  (*Henrard and Lemaître*, 1987; *Morbidelli and Moons*, 1993; *Ferraz-Mello*, 1994b; *Michtchenko and Ferraz-Mello*, 1995; *Moons et al.*, 1998). Consequently, unlike in the 3J:1, 4J:1, 5J:2, and 7J:3 MMRs, the secular dynamics do not explain why the observed orbital distribution of asteroids should display a gap at the place of the 2J:1 MMR (the Hecuba gap, see Fig. 2), where only a few tens of small resonant asteroids reside. Conversely, the 3J:2 MMR hosts some 260 resonant asteroids known at the time of writing this text (the Hilda group), with about 30 bodies exceeding 50 km in diameter.

This puzzling difference, known as the "2:1 vs. 3:2 paradox," led some authors to investigate the possibility of opening the Hecuba gap during the primordial stages of the solar system formation by invoking effects that can mutually displace the resonances and amplitudes of asteroids (*Henrard and Lemaître*, 1983). It became clear later that although plausible, such effects are not strictly required to explain the lack of asteroids in the 2J:1 MMR.

An important difference between the 2J:1 and 3J:2 MMRs was noted by *Ferraz-Mello* (1994a,b). He computed the maximum Lyapounov characteristic exponents (LCE) [the maximum LCE measures the rate of divergence of nearby orbits and is an indicator of chaos (*Benettin et al.*, 1976)] of a number of resonant orbits in both MMRs. It turned out that in the 2J:1 MMR,  $\text{LCE} \sim 10^{-5} - 10^{-3.5} \text{ yr}^{-1}$ , while in the 3J:2 MMR,  $\text{LCE} < 10^{-5.5} \text{ yr}^{-1}$ . This indicated that orbits in the 2J:1 MMR are chaotic on short timescales (*Morbidelli*, 1996), at variance with the 3J:2 MMR where most trajectories are only weakly chaotic.

The comparative study (*Nesvorný and Ferraz-Mello*, 1997) of the MMRs employing frequency map analysis (*Laskar*, 1988, 1999) provided additional clues. Plate 1 shows how the magnitude of the chaotic evolution varies in the orbital space of the 2J:1 and 3J:2 MMRs. The color coding represents the value of  $\log_{10} |\delta\bar{\omega}|$ , where  $\delta\bar{\omega}$  is the relative change of the perihelion frequency per 0.2 m.y. This quantity is a powerful indicator of the rate of chaotic evolution (chaotic diffusion) suffered by orbits in the integration timespan. The results were extrapolated to larger time intervals assuming a chaotic random walk of orbits (see *Ferraz-Mello et al.*, 1998a).

In regions corresponding to the smallest magnitudes of the chaotic diffusion (deep blue), the orbits evolve relatively by less than 10% on 1 G.y. Such orbits should be stable over the age of the solar system. Conversely, in regions where  $\log_{10} |\delta\bar{\omega}| > -2.5$  (red, yellow), the perihelion frequency of a resonant body should typically change by more than 100%

in less than 1 G.y. Such an evolution should be enough to destabilize the orbit. Thus, the orbits with  $\log_{10}|\delta\omega| > -2.5$  are expected to be unstable. Despite the large uncertainties involved in the extrapolation from million-year to billion-year timescales, Plate 1 provides a convincing argument suggesting at least 1–2 orders in magnitude shorter lifetimes in the 2J:1 than in the 3J:2 MMR. The lifetimes in the most stable regions of the 2J:1 MMR were estimated to be on the order of  $10^9$  yr (Morbidei, 1996; Nesvorný and Ferraz-Mello, 1997).

Recently, these results has been put on firmer ground by direct simulation of 50 test bodies in the 2J:1 MMR over 4 G.y. (Roig et al., 2002). This simulation showed that the most stable region of the 2J:1 MMR is characterized by marginal instabilities: There is about a 50% probability that a body started at  $3.2 < a < 3.3$  AU,  $0.2 < e < 0.4$ , small  $i$ , and  $\varpi - \varpi_J = \sigma = 0$  escapes from the resonance in 4 G.y. because of the diffusive chaos. Thus, the lack of a larger asteroid population in the 2J:1 MMR is at least partially due to the slow removal of primordial population in the last 4 G.y. The group of resonant asteroids, now accounting for some 30 small bodies known as the Zhongguo group, is localized in a very small region in the resonance where lifetimes generally exceed 4 G.y.

The origin of the Zhongguo group is unknown. This group has a steep size distribution, which would be expected from the collision injection at the breakup of the parent body of the Themis family (Morbidei, 1996). The large ejection velocities needed for such injection, an offset in  $e$  between the Themis family and the Zhongguo group, and possibly incompatible spectral type of (3789) Zhongguo, however, suggest this to be an unlikely origin (Roig et al., 2002). The Zhongguo group seems to be an order of magnitude more depleted than what would be expected from a dynamically eroded population similar to the Hilda group. Assuming Zhongguos to be dynamically primordial bodies in the 2J:1 MMR, their additional depletion could have been achieved by collision processes or during the primordial stages of the solar system formation.

The slow diffusive chaos in the 2J:1 MMR is where the concept of a resonance between an asteroid and two perturbing planets first appeared. As originally pointed out (Ferraz-Mello, 1997; Michtchenko and Ferraz-Mello, 1997; Ferraz-Mello et al., 1998b) the slow chaos in the 2J:1 MMR is probably generated by commensurabilities between the periods of the “Great Inequality,” i.e., the period of  $2\lambda_5 - 5\lambda_6$  ( $\approx 880$  yr), and of  $\sigma = 2\lambda_5 - \lambda - \varpi$  (300–500 yr). Symplectic maps of the 2J:1 MMR found the central region less chaotic when the effect of the Great Inequality was switched off. The effect of this resonance was also put into evidence in direct numerical simulations by artificially changing the Great Inequality period to 440 yr. In such situation, which could have occurred when Jupiter and Saturn were slightly closer to each other during the primordial migration phase (Fernandez and Ip, 1984), the “beat” between the periods of the Great Inequality and of  $\sigma$  was approximately 1:1, and

the instabilities in the 2J:1 MMR were significantly accelerated (inset in Plate 1). The effect of the Great Inequality may be analytically modeled as overlap between the 2J:1 and 5S:1 MMRs (Morbidei, 2002).

## 6. NUMEROUS NARROW MEAN-MOTION RESONANCES DRIVING THE CHAOTIC DIFFUSION

The narrow MMRs (three-body, high-order two-body, and resonances with Mars) in the asteroid belt are usually not powerful enough to destabilize bodies continuously resupplied into them by the Yarkovsky force (Bottke et al., 2002b) and collisions (Morbidei et al., 1995; Zappalà et al., 2000). Consequently, the narrow MMRs do not open gaps in the asteroid distribution and are populated by many asteroids at present. In the following three sections, we discuss the three-body MMRs (section 6.1), narrow two-body MMRs (section 6.2), and MMRs with Mars (section 6.3).

### 6.1. Three-Body Mean-Motion Resonances

The growing evidence that many asteroids move on chaotic orbits (Milani and Nobili, 1992; Milani and Knežević, 1994; Holman and Murray, 1996, Šidlichovský and Nesvorný, 1997; Knežević and Milani, 2000) has challenged the view of the asteroid belt as an unchanging, fossil remnant of its primordial state. For example, the asteroid 490 Veritas at  $a = 3.174$  AU has a Lyapunov time (defined as an inverse of the LCE)  $\approx 10,000$  yr, showing unpredictability of the orbit over  $>10^5$ -yr intervals. It was moreover noted that  $e$  and  $i$  of this object chaotically evolve outside the borders of the Veritas family (of which 490 Veritas is the largest fragment) in 50 m.y. Based on this fact, the age of the Veritas family was hypothesized to be of this order (Milani and Nobili, 1992).

In our current understanding, 490 Veritas is one among many objects in the asteroid belt residing in the three-body MMRs. Convincing demonstration of this fact was provided by estimates of the LCE for large samples of real and fictitious asteroids (Nesvorný and Morbidei, 1998; Murray et al., 1998; Morbidei and Nesvorný, 1999). Figure 4 shows the profile of the LCE computed for test bodies initially at  $e = 0.1$  and  $i = 0$ . The peaks correspond to chaotic regions. Some of the main peaks may be identified with two-body MMRs (3J:1 at 2.5 AU, 5J:2 at 2.82 AU, 7J:3 at 2.96 AU, etc.), while most of the narrow peaks are related to three-body MMRs. Moreover, many two-body MMRs with Mars occur in the inner asteroid belt (2.1–2.5 AU). It has been shown that a large fraction of real asteroids reside in narrow resonances (Nesvorný and Morbidei, 1998). 490 Veritas evolves in the 5J:–2S:–2, the angle  $\sigma_{5,-2,-2,0,0,-1,0,0,0}$  having irregular oscillations about 0 correlated with oscillations of semimajor axis about  $a_{\text{res}} = 3.174$  AU.

This result raised questions concerning the implications of such a complex chaotic structure of the asteroid belt.

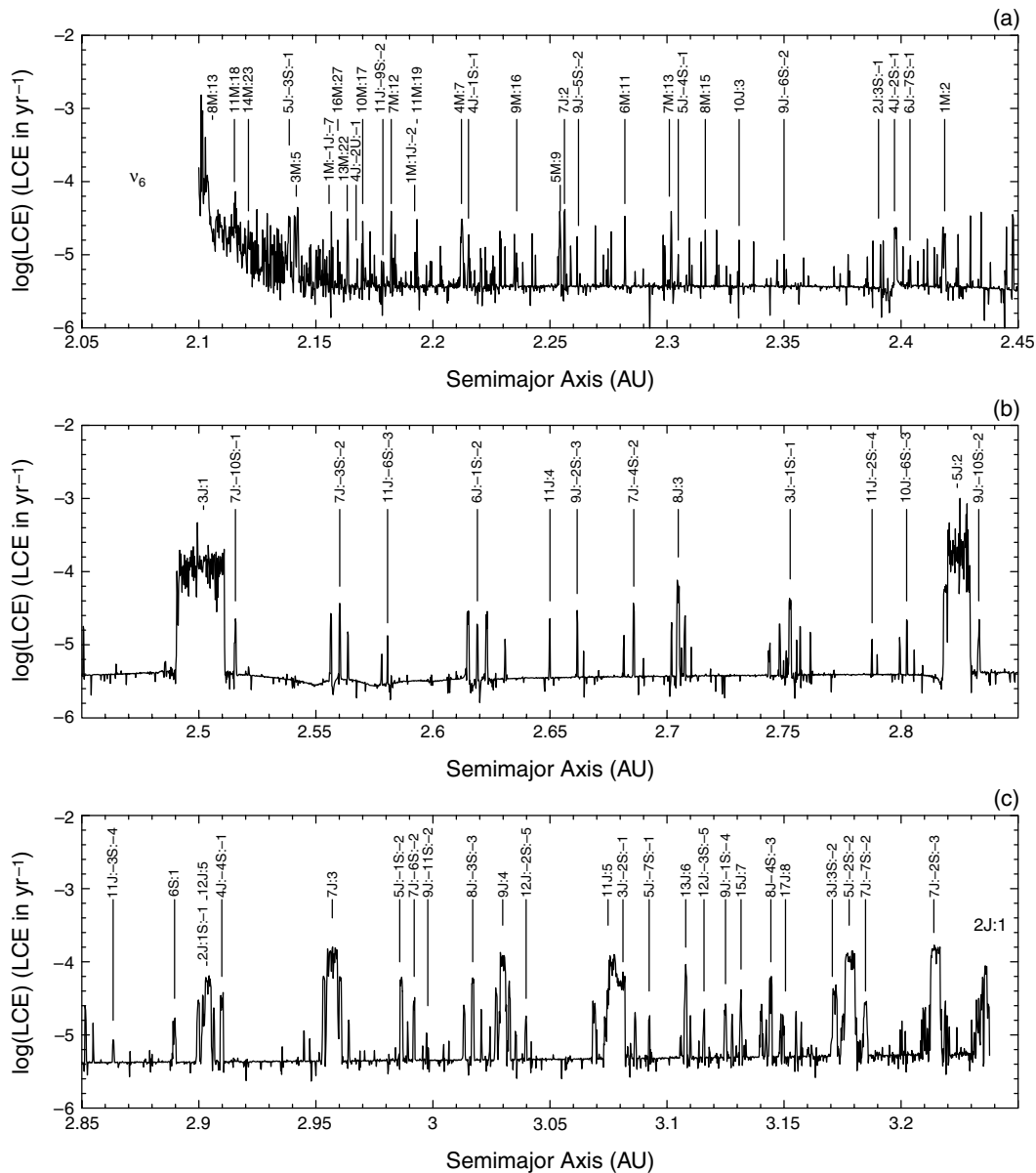


**Fig. 4.** The estimate of the LCE computed for test bodies initially placed on a regular grid in semimajor axis, with  $e = 0.1$ . (a) The gravitational perturbations provided by the terrestrial planets were taken into account in addition to the perturbations of four giant planets. (b,c) Accounted only for four giant planets. The figure shows many peaks that rise from a background level. The background value of about  $10^{-5.3} \text{ yr}^{-1}$  is dictated by the limited integration timespan (2.2 m.y.); increasing the latter, the background level generally decreases. The peaks reveal the existence of narrow chaotic regions associated with MMRs. The main resonances are indicated above the corresponding peaks. From *Morbidelli and Nesvorný* (1999).

Asteroids were shown to escape from the main belt to Mars- and Jupiter-crossing orbits due to a slow chaotic evolution of eccentricities in narrow resonances. Realistic modeling including the Yarkovsky effect demonstrated that the narrow resonances are an important source of the near-Earth-object population (*Migliorini et al.*, 1998; *Morbidelli and Nesvorný*, 1999; *Botke et al.*, 2002a). Recently, narrow MMRs were also hypothesized to disperse the asteroid families in  $e$  and  $i$ , possibly creating their often asymmetric shapes (*Nesvorný et al.*, 2002). If this process is as general as con-

jectured, many asteroid families could have been created as small groupings and later were dynamically dispersed by chaotic diffusion in narrow MMRs and by the Yarkovsky effect. This mechanism may eventually solve the paradox between hydrocode simulations of breakup events suggesting creation of tightly grouped collision swarms, and the observed, largely dispersed asteroid families.

Theoretical modeling of the three-body MMRs revealed several clues to understanding the behavior of asteroids in numerical simulations. The resonant Hamiltonian of sev-

eral three-body MMRs with Jupiter and Saturn in the planar model has been computed by *Murray et al.* (1998) and by *Nesvorný and Morbidelli* (1999). Following the notation of the latter work, the Hamiltonian of the  $k_5J:k_6S:k$  MMRs (equation (10)) can be written as a Fourier expansion

$$\bar{\mathcal{H}}_1 = \frac{1}{a_5} \sum_{\mathbf{v}} \mathcal{P}_{1,\mathbf{v}}(\alpha_{\text{res}}) e_5^{s_5} e_6^{s_6} e^s \cos[l_5 \varpi_5 + l_6 \varpi_6 - l(\sigma + \nu)] \quad (17)$$

$$\bar{\mathcal{H}}_2 = \frac{1}{a_5} \sum_{\mathbf{v}} \mathcal{P}_{2,\mathbf{v}}(\alpha_{\text{res}}) e_5^{s_5} e_6^{s_6} e^s \cos[\sigma_{\mathbf{k},\mathbf{k},(l_5,l_6),l,0,0}]$$

where  $\alpha_{\text{res}} = a_{\text{res}}/a_5$ , and the multiindex  $\mathbf{v}$  denotes different values of integers  $s_5, s_6, s, l_5, l_6, l$ . The angle  $\sigma_{\mathbf{k},\mathbf{k},(l_5,l_6),l,0,0}$  in equation (17) is given in terms of  $\sigma$  and  $\nu$  (equation (7)). Denoting

$$\beta = \frac{\mu_5^2}{a_5} \sum_{\substack{\mathbf{v} \\ l_5=l_6=0}} \mathcal{P}_{2,\mathbf{v}} e^s \quad (18)$$

these coefficients, truncated at two lowest orders in  $e$ , are given in Table 1.

Ignoring all but one resonant multiplet term in equation (17) (generically denoted by  $\sigma_*$ ), the complete Hamiltonian equation (10) can be reduced to the Hamiltonian of a simple pendulum  $\mathcal{H} = \alpha(S - N)^2 + \beta \cos \sigma_*$ ,  $N$  representing a constant parameter (*Nesvorný and Morbidelli*, 1999; *Murray et al.*, 1998). The resonant full width can then be computed from equation (11). Similarly, the period of small

amplitude librations (in years) is

$$T = \frac{a_{\text{res}}}{|k|} \sqrt{\frac{1}{3\beta}} \quad (19)$$

The position of the libration center  $\sigma_c$  is determined by the signs of  $\alpha$  and  $\beta$ . As  $\alpha = -3\lambda^2/2a_{\text{res}}^2$  is always negative, the resonant center is at 0 when  $\beta > 0$ , and at  $\pi$  when  $\beta < 0$ . Moreover, according to simple arguments, the Lyapunov time is on the order of the libration period, so that  $T$  provides a rough estimate of the LCE (*Benettin and Gallavotti*, 1986; *Holman and Murray*, 1996).

Table 1 shows  $\Delta a$ ,  $T$ , and  $\sigma_c$  for the most important three-body MMRs with  $e = 0.1$ . The values computed from equations (11) and (19) are in good agreement with numerical results (Fig. 4). In particular, 490 Veritas was numerically found to evolve in the 5J:−2S:−2 MMR with 0.004-AU oscillations of  $a$  and the libration period of several  $10^3$  yr, both values being in agreement with the ones in Table 1.

Understanding the chaos and the long-term evolution of asteroids in the three-body MMRs requires to account for more than one multiplet term in equation (17). *Murray et al.* (1998) and *Nesvorný and Morbidelli* (1999) showed that different multiplets of the three-body MMR generally overlap, thus creating a chaotic domain at the position of the MMR. Quantitative estimates of the LCE and diffusion timescales in this domain showed that significant chaotic evolutions of  $e$  and  $i$  of resonant bodies occur on long timespans (*Murray and Holman*, 1997; *Murray et al.*, 1998). Conversely, the semimajor axis of resonant bodies remains

TABLE 1. Analytic results on the three-body MMRs (from *Nesvorný and Morbidelli*, 1999).

Resonance Designation	Resonant Semimajor Axis $a_{\text{res}}$ (AU)	Coefficient $\beta$ ( $\times 10^{-8}$ )	Resonance Width ( $e = 0.1$ )	Libration Period $T$ ( $10^3$ yr) ( $e = 0.1$ )	Libration Center $\sigma_c$
4J:−1S:−1	2.2155	$6.05e^2 - 2.22e^4$	0.37	52	0
3J: 1S:−1	2.2994	$3.78e^3 - 1.94e^5$	0.1	217	0
4J:−2S:−1	2.3978	$19.7e - 3.95e^3$	2.4	9.9	0
7J:−2S:−2	2.4479	$46.0e^3 - 53.0e^5$	0.37	33	0
7J:−3S:−2	2.5600	$-4.35e^2 + 5.28e^4$	0.39	36	$\pi$
2J: 2S:−1	2.6155	$6.03e^3 + 3.63e^5$	0.15	200	0
6J:−1S:−2	2.6192	$-17.6e^3 + 21.3e^5$	0.25	57	$\pi$
4J:−3S:−1	2.6229	$-0.206 - 0.763e^2$	0.9	30	$\pi$
7J:−4S:−2	2.6858	$0.255e - 0.356e^3$	0.3	49	0
3J:−1S:−1	2.7527	$-7.99e + 0.360e^3$	1.9	17.8	$\pi$
4J:−4S:−1	2.9092	$0.0203e + 0.0691e^3$	0.1	370	0
5J:−1S:−2	2.9864	$20.9e^2 - 21.3e^4$	1.1	19	0
8J:−3S:−3	3.0166	$-10.0e^2 + 24.0e^4$	0.8	19	$\pi$
3J:−2S:−1	3.0794	$-3.06 - 15.5e^2$	4.5	9.9	$\pi$
6J: 1S:−3	3.1389	$-22.4e^4 + 143e^6$	0.12	132	$\pi$
8J:−4S:−3	3.1421	$0.357e - 0.99e^3$	0.5	33	0
3J: 3S:−2	3.1705	$-25.8e^4 + 5.15e^6$	0.13	180	$\pi$
5J:−2S:−2	3.1751	$45.6e - 32.3e^3$	5.6	4.3	0
7J:−2S:−3	3.2100	$-115e^2 + 273e^4$	2.8	5.8	$\pi$

locked in the interval spanned by the resonant multiplet and although behaving stochastically on short timespans, never directly evolves outside the resonant borders, unless two or more different MMRs overlap (the case of high  $e$  in Fig. 2).

## 6.2. Narrow Two-Body Mean-Motion Resonances with Jupiter

As discussed above, the details of the multiplet structure of each two-body and three-body resonance affect the extent of the chaotic zone associated with the resonance, the typical Lyapunov time for a small body in that resonance, and the timescale on which such a body might chaotically diffuse in the space of orbital elements. Useful analytic models of these effects can be obtained using some simplifying assumptions (*Holman and Murray, 1996; Murray and Holman, 1997; Murray et al., 1998*). We show an example of such modeling for a two-body resonance (see also *Morbidelli, 2002*). This modeling can be used with small modifications for the three-body (*Nesvorný and Morbidelli, 1999*) and Mars' MMRs.

To most simply account for the multiplet structure of a two-body ( $\mathbf{k}, \mathbf{k}$ ) MMR, we restrict ourselves to the planar elliptic three-body model. The resonant Hamiltonian of such model can be written

$$\mathcal{H} = -\frac{1}{2\Lambda^2} + \frac{k_{j_1}}{k} n_{j_1} \Lambda + c_0(\Lambda, \mathbf{P}) + \sum_{s=0}^{|k_{j_1} + k|} c_s(\Lambda, \mathbf{P}) \times \cos\left[k_{j_1} \lambda_{j_1} + k\lambda + s\phi - (k_{j_1} + k - s)\varpi_{j_1}\right] \quad (20)$$

where  $c_0$  is a part of  $\mu\bar{\mathcal{H}}_1$  in equation (8) independent of angles. In equation (20), we retained only those terms of the Fourier expansion of equation (8) that are lowest order in the eccentricities of the planet and the small body. For simplicity, we arbitrarily set  $\varpi_{j_1} = 0$ , and drop it from equation (20).

The canonical variables we use in the following slightly differ from equation (7). We define them by

$$\begin{aligned} \Psi &= k_{j_1} \lambda_{j_1} + k\lambda & \Psi &= \frac{1}{k}(\Lambda - \Lambda_0) \\ \phi &= p & I &= P \\ \lambda_{j_1} & & \tilde{\Lambda}_{j_1} &= \Lambda_{j_1} - \frac{k_{j_1}}{k} \Lambda \end{aligned} \quad (21)$$

where  $\Lambda_0 = \sqrt{a_{\text{res}}}$  is the unperturbed MMR location. Keeping the lowest-order terms in  $\Psi$  and  $I$  in the Taylor expansion of first three terms of Hamiltonian equation (20), we get

$$\mathcal{H} = \frac{1}{2}\beta\Psi^2 + 2\varepsilon AI + \sum_{s=0}^{|k_{j_1} + k|} c_s(I) \cos(\Psi + s\phi) \quad (22)$$

where  $\beta$  and  $2\varepsilon A = \partial c_0 / \partial I(\Lambda_0, 0)$  are the constants associated with the Taylor expansion, and  $c_s(I) = c_s(\Lambda_0, I)$ .

To apply the resonance overlap criterion to the Hamiltonian equation (22) we must compute the separation and

widths of the individual multiplet terms in the resonance. The separation in  $\Psi$  between two such terms is given by  $\beta\delta\Psi = 2\varepsilon A$ , while the width of each multiplet is  $\Delta\Psi = 2\sqrt{c_s(I, P_{j_1})/\beta}$ . The stochasticity parameter (*Chirikov, 1979; Lichtenberg and Lieberman, 1983*) is then

$$K_{\text{eff}} = \left(\pi \frac{\Delta\Psi}{\delta\Psi}\right)^2 = \left(\frac{c_{s_0}}{\beta}\right) \left(\frac{\pi\beta}{\varepsilon A}\right)^2 \quad (23)$$

where  $c_{s_0}$  is the coefficient of a representative multiplet term (*Murray and Holman, 1997*). The orbits in the MMR will be chaotic if  $K_{\text{eff}} > K_{\text{crit}}$ , where  $K_{\text{crit}} \sim 1$ . The extent of the chaotic zone in  $\Psi$  (and therefore in semimajor axis) is roughly given by the  $\Psi$  range of those multiplet terms that overlap. The Lyapunov time in the chaotic zone is given by

$$T_L \approx \frac{\pi}{\varepsilon A} / \ln \left[ 1 + \frac{K_{\text{eff}}}{4} + \sqrt{\frac{K_{\text{eff}}}{2} + \left(\frac{K_{\text{eff}}}{4}\right)^2} \right] \sim \frac{\pi}{\varepsilon A} \quad (24)$$

which indicates that the Lyapunov time is comparable to the precession period.

If  $K_{\text{eff}} > K_{\text{crit}}$ , the diffusion in  $\Psi$  and  $I$ , can be described by the Fokker-Planck equation (*Lichtenberg and Lieberman, 1983; Murray and Holman, 1997*). The associated diffusion coefficients are

$$D_\Psi \approx \frac{K_{\text{eff}}^2}{2} \left(\frac{\varepsilon A}{\pi\beta}\right)^2 = \frac{1}{2} \left(\frac{c_{s_0}}{\beta}\right)^2 \left(\frac{\pi\beta}{\varepsilon A}\right)^2 = \frac{1}{2} c_{s_0}^2 \frac{\pi}{\varepsilon A} \quad (25)$$

and

$$D_I = s_0^2 D_\Psi = \frac{s_0^2}{2} c_{s_0}^2 \frac{\pi}{\varepsilon A} \quad (26)$$

In the model of *Murray and Holman (1997)* the resonant bodies execute random walks in  $\Psi$  (or semimajor axis) and  $I$  (or eccentricity). These random walk are subject to boundary conditions. The permissible values of  $\Psi$  lie within the range of values for which the resonant multiplet terms overlap (the chaotic zone). The values of  $I$  range from  $I = 0$  (circular orbit) to  $I = I_{\text{max}}$ , where  $I_{\text{max}}$  corresponds to planet crossing. The bounding values of  $\Psi$  and  $I = 0$  can be modeled as reflecting barriers, and the value of  $I = I_{\text{max}}$  as an absorbing barrier. For a resonant asteroid at  $I_0$ , the solution of the Fokker-Planck equation yields typical values of the removal time,  $T_R$ , of

$$T_R \sim \frac{I_{\text{max}} I_0}{\sqrt{D_I(I_{\text{max}}) D_I(I_0)}} \quad (27)$$

Figure 5 shows removal times for outer-belt asteroids in a number of two-body MMRs. The solid symbols are the results of numerical integrations; the open symbols are analytic predictions from equation (27). The values of  $I_0$  were determined from short numerical integrations of resonant asteroids, hence the scatter in the predicted removal

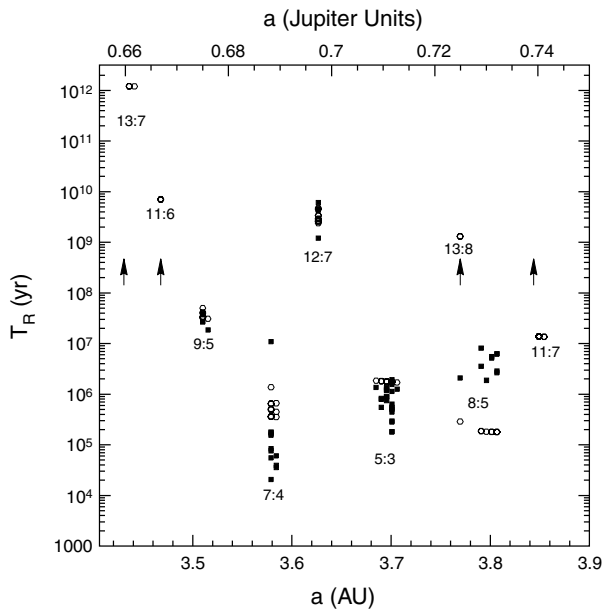


**Fig. 5.** The removal times for outer-belt asteroids in a number of two-body MMRs with Jupiter. The solid symbols are the results of numerical integrations; the open symbols are analytic predictions from equation (27). The arrows represent lower limits obtained from numerical integration of bodies in MMRs characterized by extremely slow chaotic diffusion. Here, Jupiter units are 5.2 AU. From *Murray and Holman (1997)*.

times. In most cases the results of numerical experiments agree with the analytic predictions to an order of magnitude. The results of these calculations indicate that for high-order MMRs in the outer belt, removal times are in some MMRs substantially shorter than the age of the solar system (the case of the 7J:4, 5J:3, and 8J:5 MMRs) and in other resonances substantially longer than the age of the solar system (the 13J:7 and 11J:6 MMRs).

Figure 5 shows that resonances like the 7J:4, 5J:3, and 8J:5 MMR are expected to correspond to gaps in the asteroid distribution. Indeed, no large outer-belt asteroids are observed in them (Fig. 2). The outer asteroid belt, however, seems more depleted than what would be expected from the effect of chaotic resonances. This led some authors to suggest that depletion occurred during the primordial radial migration of the planets (*Holman and Murray, 1996; Liou and Malhotra, 1997*). The same scenario can also nicely explain the presence of many asteroids in the 3J:2 MMR, which could have been captured by the resonance accompanying the inward migration of the Jupiter. Alternatively, the outer asteroid belt could have been depleted by the effect of large Jupiter-scattered planetesimals (*Petit et al., 1999*).

### 6.3. Mean-Motion Resonances with Mars

It may seem surprising at a first glance that the MMRs with Mars are important in the asteroid belt because Mars

is a factor of  $\approx 3000$  less massive than Jupiter. Thus, according to the discussion in section 2, the two-body MMRs with Mars should be in general a factor  $\sqrt{3000} \sim 55$  smaller than the two-body MMRs with Jupiter. In the inner asteroid belt, however, this factor may be compensated for by the small distance between an asteroid and Mars. Indeed, the width of any MMRs near the planet-crossing limit becomes large. According to Fig. 2 (see also Fig. 4), the MMRs with Mars provide a dominant source of chaos in the inner asteroid belt, overwhelming in size and number the MMRs with Jupiter.

The dynamical interaction of asteroids with the MMRs with Mars is complex. As an example, Fig. 5 shows the evolution of  $a$ ,  $\sigma = 9\lambda_4 - 22\lambda + 13\bar{\omega}$ , and  $e^{13/2}$  of 41 Daphne. This asteroid is temporally captured in the 3M:11 MMR when  $e$  becomes large during the secular oscillations. The irregular behavior of  $a$  and  $\sigma$  witnesses the chaoticity of the orbit, which has a Lyapunov time of  $< 10^4$  yr (*Šidlichovský, 1999*).

Very little analytical work has been done on the subject of the MMRs with Mars. Figures 1e–f are apparently highly idealized approximations of the real dynamics (Fig. 6). To understand the real dynamics, it is important to account for the rich multiplet structure of the MMRs with Mars and the significant time-modulation of each multiplet’s width with varying eccentricities (interesting MMRs with Mars are usually of a very high order).

The chaotic diffusion in the MMRs with Mars provide transfer routes from the asteroid belt to Mars-crossing orbits. This source was hypothesized to be one of the major sources of large NEAs (*Migliorini et al., 1998; Morbidelli and Nesvorný, 1999; Bottke et al., 2002a*). The detailed mechanism of this transfer involves the complex interaction of the Yarkovsky effect and MMRs. In particular, the Yarkovsky effect is thought to be responsible for refilling MMRs by new objects; otherwise the space occupied by the active MMRs would be cleared of the asteroids, and gaps in the asteroid distribution at resonant semimajor axes would be created. Such gaps are not currently observed.

## 7. PERSPECTIVES

In the last decade, we witnessed fascinating progress from studies of separate MMRs in simplest physical models to the global understanding of the structure and effects of MMRs throughout the asteroid belt. Nevertheless, we feel that many open problems await solution. The least developed is the modeling of narrow resonances, especially the three-body MMRs and the MMRs with Mars. The intricate interaction of MMRs and the Yarkovsky effect is an interesting subject for future studies.

Basically, one would like to know how the probability of capture of a drifting body into narrow MMRs depends on the magnitude and direction of the semimajor axis drift, and whether the phase of secular angles plays any role in the capture process. Ideally, when capture occurs, one would also like to statistically estimate the change of  $e$  and  $i$  of an asteroid during the time spent on a resonant orbit. Although some hints about these processes may be derived from re-

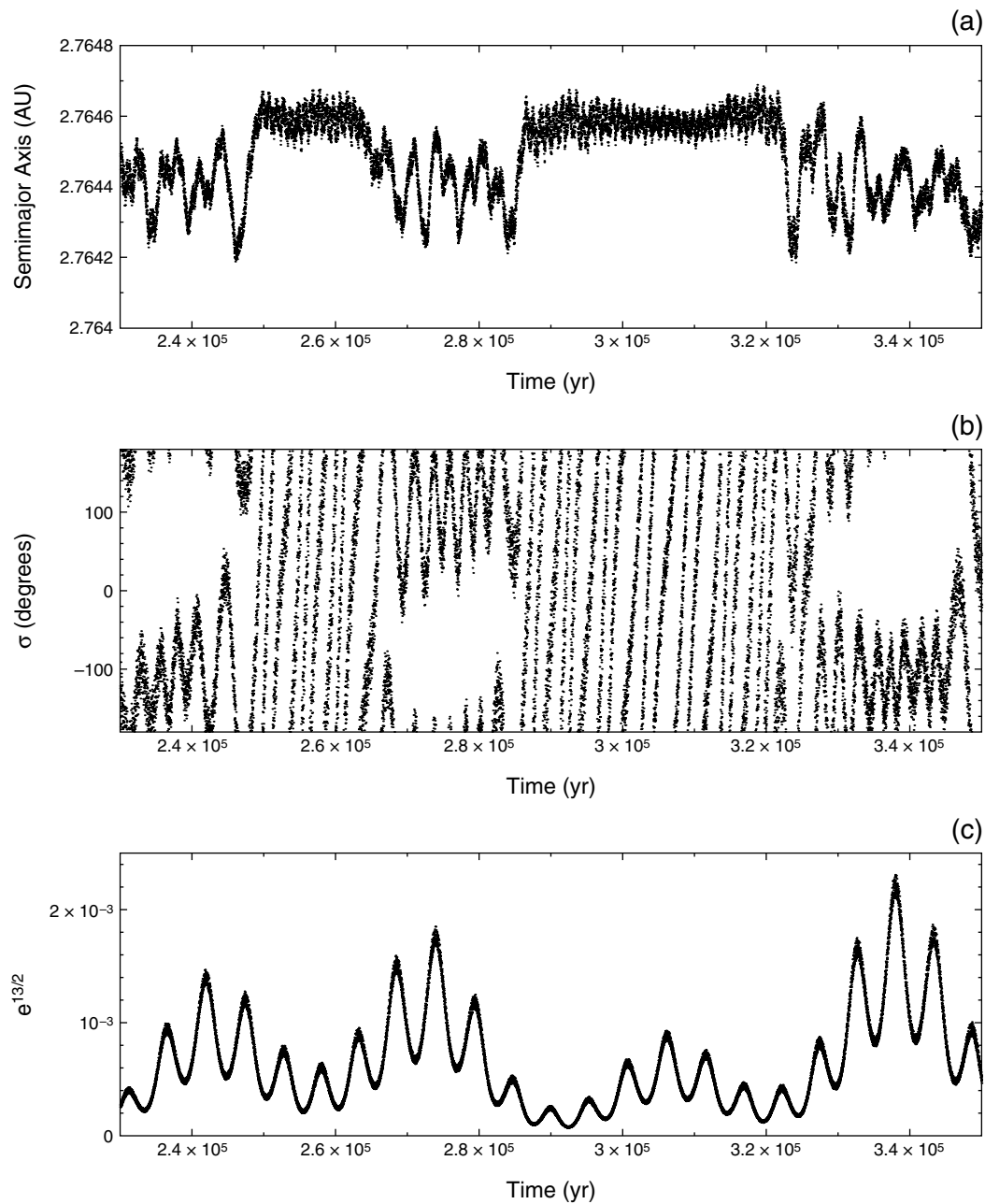


**Fig. 6.** The evolution of orbital elements of the asteroid 41 Daphne. The panels show (a) the semimajor axis, (b)  $\sigma = 9\lambda_4 - 22\lambda + 13\varpi$ , and (c)  $e^{13/2}$ . The evolution of 41 Daphne is characterized by the interaction with the 9M:22 MMR. The width of a MMR is proportional to  $e^{\rho/2}$  (see equation (11) and related discussion), where here  $\rho = 13$ . Consequently, the resonant width seen by the asteroid is largely modulated with the parameter in (c). Resonant behavior occurs only when the eccentricity of 41 Daphne is large. Adapted from Šidlichovský (1999).

cent numerical simulations, the general trends in the parameter space are unknown. Yet the interaction of narrow MMRs with the Yarkovsky effect is important for such issues as the origin of NEAs and the dynamical dispersion of the asteroid families. Also remaining are a few puzzles concerning the asteroid population of large MMRs in the asteroid belt, possibly related to the processes involved in the early stages of the solar system formation.

We note that a large number of asteroids exist in the 3J:2 MMR, while both the 2J:1 and 4J:3 MMRs are substantially depleted. Although some depletion of latter resonances can be explained by the chaotic processes acting in the last 4 b.y., additional depopulation likely occurred during the formation of the asteroid belt. Is the resonant structure of the outer asteroid belt a natural outcome of the accretion itself (*Petit et al.*, 1999), or possibly a sign of the primor-

dial planetary migration? We wonder if a unique answer to this question can be given. Apparently, detailed modeling of the primordial phases is required.

Such quantitative modeling should also show whether the current depletion of the outer belt between the 2J:1 and 3J:2 MMRs (3.4–3.9 AU) requires primordial migration (Holman and Murray, 1996; Liou and Malhotra, 1997). Moreover, what effect would planetary migration have in the primordial main asteroid belt? First attempts to quantify this effect by direct simulations (Gomes, 1997; Levison et al., 2001) show that the sweeping  $v_6$  secular resonance is efficient at deleting the asteroid population. Our hope is that the increasingly detailed information about the current asteroid belt provided by observations, combined with future progress in theoretical modeling, will further reveal signatures that primordial processes imprinted on the orbital structure of the belt, and that have been preserved until now. Understanding the effects of MMRs will certainly be part of that story.

## REFERENCES

- Beaugé C. (1994) Asymmetric librations in exterior resonances. *Cel. Mech. Dyn. Astron.*, 60, 225–248.
- Benettin G. and Gallavotti G. (1986) Stability of motions near resonances in quasi-integrable Hamiltonian systems. *J. Stat. Phys.*, 44, 293–338.
- Benettin G., Galgani L., and Strelcyn J. (1976) Kolmogorov entropy and numerical experiments. *Phys. Rev. A.*, 14, 2338–2345.
- Bretagnon P. and Simon J.-L. (1990) General theory of the Jupiter-Saturn pair using an iterative method. *Astron. Astrophys.*, 239, 387–398.
- Bottke W. F., Morbidelli A., Jedicke R., Petit J.-M., Levison H., Michel P., and Metcalfe T. S. (2002a) Debaised orbital and size distributions of the Near-Earth Objects. *Icarus*, in press.
- Bottke W. F. Jr., Vokrouhlický D., Rubincam D. P., and Brož M. (2002b) The effect of Yarkovsky thermal forces on the dynamical evolution of asteroids and meteoroids. In *Asteroids III* (W. F. Bottke Jr. et al., eds.), this volume. Univ. of Arizona, Tucson.
- Bowell E. K., Muinonen K., and Wasserman L. H. (1994) A public-domain asteroid orbit database. In *Asteroids, Comets and Meteors* (A. Milani et al., eds.), pp. 477–481. Kluwer, Dordrecht.
- Chirikov B. V. (1979) A universal instability of many-dimensional oscillator systems. *Phys. Rep.*, 52, 263–379.
- Dermott S. F. and Murray C. D. (1983) Nature of the Kirkwood gaps in the asteroid belt. *Nature*, 301, 201–205.
- Farinella P., Froeschlé C., and Gonczi R. (1993) Meteorites from the asteroid 6 Hebe. *Cel. Mech. Dyn. Astron.*, 56, 287–305.
- Farinella P., Froeschle C., Froeschle C., Gonczi R., Hahn G., Morbidelli A., and Valsecchi G. B. (1994) Asteroids falling onto the Sun. *Nature*, 371, 315–317.
- Fernandez J. A. and Ip W.-H. (1984) Some dynamical aspects of the accretion of Uranus and Neptune — The exchange of orbital angular momentum with planetesimals. *Icarus*, 58, 109–120.
- Ferraz-Mello S. (1994a) Kirkwood gaps and resonant groups. *IAU Symp.* 160, pp. 175–188.
- Ferraz-Mello S. (1994b) The dynamics of the asteroidal 2:1 resonance. *Astron. J.*, 108, 2330–2337.
- Ferraz-Mello S. (1997) A symplectic mapping approach to the study of the stochasticity in asteroidal resonances. *Cel. Mech. Dyn. Astron.*, 65, 421–437.
- Ferraz-Mello S. and Klafke J. C. (1991) A model for the study of very-high-eccentricity asteroidal motion. The 3:1 resonance. In *Predictability, Stability and Chaos in N-Body Dynamical Systems* (A. E. Roy, ed.), pp. 177–184. NATO Adv. Stud. Inst. Ser. B Phys. 272, Plenum, New York.
- Ferraz-Mello S., Nesvorný D., and Michtchenko T. A. (1998a) Chaos, diffusion, escape and permanence of resonant asteroids in gaps and groups. In *Solar System Formation and Evolution* (D. Lazzaro et al., eds.), pp. 65–82. ASP Conference Series 149.
- Ferraz-Mello S., Michtchenko T. A., and Roig F. (1998b) The determinat role of Jupiter’s Great Inequality in the depletion of the Hecuba gap. *Astron. J.*, 116, 1491–1500.
- Gladman B.J., Migliorini F., Morbidelli A., Zappalà V., Michel P., Cellino A., Froeschlé C., Levison H. F., Mailey M., and Duncan M. (1997) Dynamical lifetimes of objects injected into asteroid belt resonances. *Science*, 277, 197–201.
- Gomes R. S. (1997) Dynamical effects of planetary migration on the primordial asteroid belt. *Astron. J.*, 114, 396–401.
- Henrard J. (1990) A semi-numerical perturbation method for separable Hamiltonian systems. *Cel. Mech. Dyn. Astron.*, 49, 43–67.
- Henrard J. and Lemaître A. (1983) A mechanism of formation for the Kirkwood gaps. *Icarus*, 55, 482–494.
- Henrard J. and Lemaître A. (1987) A perturbative treatment of the 2/1 Jovian resonance. *Icarus*, 69, 266–279.
- Henrard J., Watanabe N., and Moons M. (1995) A bridge between secondary and secular resonances inside the Hecuba gap. *Icarus*, 115, 336–346.
- Holman M. J. and Murray N. W. (1996) Chaos in high-order mean resonances in the outer asteroid belt. *Astron. J.*, 112, 1278.
- Hori G. (1966) Theory of general perturbation with unspecified canonical variable. *Publ. Astron. Soc. Japan*, 18, 287.
- Jedicke R. and Metcalfe T.S. (1998) The orbital and absolute magnitude distributions of main belt asteroids. *Icarus*, 113, 245–260.
- Klafke J. C., Ferraz-Mello S., and Michtchenko T. (1992) Very-high-eccentricity librations at some higher-order resonances. *IAU Symp.* 152, pp. 153–158.
- Knežević Z. and Milani A. (2000) Synthetic proper elements for outer main belt asteroids. *Cel. Mech. Dyn. Astron.*, 78, 17.
- Laskar J. (1988) Secular evolution of the solar system over 10 million years. *Astron. Astrophys.*, 198, 341–362.
- Laskar J. (1999) Introduction to frequency map analysis. In *Hamiltonian Systems with Three or More Degrees of Freedom* (C. Simó, ed.), pp. 134–150. Kluwer, Dordrecht.
- Lecar M., Franklin F. A., Holman M. J., and Murray N. W. (2001) Chaos in the solar system. In *Annu. Rev. Astron. Astrophys.*, 39, 581–631.
- Levison H. F. and Duncan M. J. (1994) The long-term dynamical behavior of short-period comets. *Icarus*, 108, 18–36.
- Levison H. F., Dones L., Chapman C. R., Stern S. A., Duncan M. J., and Zahnle K. (2001) Could the lunar “Late Heavy Bombardment” have been triggered by the formation of Uranus and Neptune? *Icarus*, 151, 286–306.
- Lichtenberg A. J. and Leiberman M. A. (1983) *Regular and Stochastic Motion: Applied Mathematical Sciences, Vol. 38*. Springer, New York.
- Liou J. C. and Malhotra R. (1997) Depletion of the outer asteroid belt. *Science*, 275, 375–377.

- Message P. J. (1958) Proceedings of the Celestial Mechanics Conference: The search for asymmetric periodic orbits in the restricted problem of three bodies. *Astron. J.*, *63*, 443.
- Michtchenko T. A. and Ferraz-Mello S. (1995) Comparative study of the asteroidal motion in the 3:2 and 2:1 resonances with Jupiter — I. *Astron. Astrophys.*, *303*, 945–963.
- Michtchenko T. A. and Ferraz-Mello S. (1997) Escape of asteroids from the Hecuba gap. *Planet. Space Sci.*, *45*, 1587–1593.
- Migliorini F., Michel P., Morbidelli A., Nesvorný D., and Zappalà V. (1998) Origin of multikilometer Earth and Mars-crossing asteroids: A quantitative simulation. *Science*, *281*, 2022–2024.
- Milani A. and Knežević Z. (1994) Asteroid proper elements and the dynamical structure of the asteroid main belt. *Icarus*, *107*, 219–254.
- Milani A. and Nobili A. M. (1992) An example of stable chaos in the solar system. *Nature*, *357*, 569–571.
- Milani A., Nobili A. M., and Knežević Z. (1997) Stable chaos in the asteroid belt. *Icarus*, *125*, 13–31.
- Moons M. (1993) On the resonant Hamiltonian in the restricted three-body problem. *Internal Report, 19*, Facultés Universitaires de Namur, Belgique.
- Moons M. and Morbidelli A. (1995) Secular resonances in mean-motion commensurabilities. The 4/1, 3/1, 5/2 and 7/3 cases. *Icarus*, *114*, 33–50.
- Moons M., Morbidelli A., and Migliorini F. (1998) Dynamical structure of the 2/1 commensurability with Jupiter and the origin of the resonant asteroids. *Icarus*, *135*, 458–468.
- Morbidelli A. (1996) The Kirkwood Gap at the 2/1 commensurability with Jupiter: New numerical results. *Astron. J.*, *111*, 2453.
- Morbidelli A. (2002) *Modern Celestial Mechanics. Aspects of the Solar System Dynamics*. Gordon and Breach, London, in press.
- Morbidelli A. and Moons M. (1993) Secular resonances in mean-motion commensurabilities. The 2/1 and 3/2 cases. *Icarus*, *102*, 316–332.
- Morbidelli A. and Moons M. (1995) Numerical evidences of the chaotic nature of the 3/1 mean-motion commensurability. *Icarus*, *115*, 60–65.
- Morbidelli A. and Nesvorný D. (1999) Numerous weak resonances drive asteroids toward terrestrial planets orbits. *Icarus*, *139*, 295–308.
- Morbidelli A., Zappalà V., Moons M., Cellino A., and Gonczi R. (1995) Asteroid families close to mean-motion resonances: Dynamical effects and physical implications. *Icarus*, *118*, 132–154.
- Morbidelli A., Bottke W. F. Jr., Froeschlé Ch., and Michel P. (2002) Origin and evolution of near-Earth objects. In *Asteroids III* (W. F. Bottke Jr. et al., eds.), this volume. Univ. of Arizona, Tucson.
- Murray N. and Holman M. (1997) Diffusive chaos in the outer belt. *Astron. J.*, *114*, 1246–1259.
- Murray N., Holman M., and Potter M. (1998) On the origin of chaos in the solar system. *Astron. J.*, *116*, 2583–2589.
- Nesvorný D. and Ferraz-Mello S. (1997) On the asteroidal population of the first-order resonances. *Icarus*, *130*, 247–258.
- Nesvorný D. and Morbidelli A. (1998) Three-body mean-motion resonances and the chaotic structure of the asteroid belt. *Astron. J.*, *116*, 3029–3037.
- Nesvorný D. and Morbidelli A. (1999) An analytic model of three-body mean motion resonances. *Cel. Mech. Dyn. Astron.*, *71*, 243–263.
- Nesvorný D., Morbidelli A., and Vokrouhlický D., Bottke W. F., Brož M. (2002) The Flora family: A case of the dynamically dispersed collisional swarm? *Icarus*, *157*, 155–172.
- Petit J., Morbidelli A., and Valsecchi G. B. (1999) Large scattered planetesimals and the excitation of the small body belts. *Icarus*, *141*, 367–387.
- Roig F., Nesvorný D., and Ferraz-Mello S. (2002) Asteroids in the 2:1 resonance with Jupiter. Dynamics and size distribution. *Mon. Not. R. Astron. Soc.*, in press.
- Saha P. (1992) Simulating the 3:1 Kirkwood gap. *Icarus*, *100*, 434–439.
- Šidlichovský M. (1999) On stable chaos in the asteroid belt. *Cel. Mech. Dyn. Astron.*, *73*, 77–86.
- Šidlichovský M. and Nesvorný D. (1997) Frequency modified Fourier transform and its applications to asteroids. *Cel. Mech. Dyn. Astron.*, *65*, 137–148.
- Wisdom J. (1980) The resonance overlap criterion and the onset of stochastic behavior in the restricted three-body problem. *Astron. J.*, *85*, 1122–1133.
- Wisdom J. (1982) The origin of Kirkwood gaps: A mapping for asteroidal motion near the 3/1 commensurability. *Astron. J.*, *85*, 1122–1133.
- Wisdom J. (1983) Chaotic behaviour and the origin of the 3/1 Kirkwood gap. *Icarus*, *56*, 51–74.
- Wisdom J. (1985) Meteorites may follow a chaotic route to earth. *Nature*, *315*, 731–733.
- Wisdom J. and Holman M. (1991) Symplectic maps for the N-body problem. *Astron. J.*, *102*, 1528–1538.
- Yoshikawa M. (1990) Motions of asteroids at the Kirkwood gaps. I — On the 3:1 resonance with Jupiter. *Icarus*, *87*, 78–102.
- Yoshikawa M. (1991) Motions of asteroids at the Kirkwood Gaps. II — On the 5:2, 7:3, and 2:1 resonances with Jupiter. *Icarus*, *92*, 94–117.
- Zappalà V., Bendjoya P., Cellino A., Di Martino M., Doressoundiram A., Manara A., and Migliorini F. (2000) Fugitives from the Eos family: First spectroscopic confirmation. *Icarus*, *145*, 4–11.